11.2 ESTIMATES OF AIR AND POLLUTANT EXCHANGE FOR STREET CANYONS IN COMBINED WIND-BUOYANCY DRIVEN FLOW USING THE RANS RENORMALIZATION GROUP *k-ε* TURBULENCE MODEL

Chun-Ho Liu*, Wai Chi Cheng and Dennis Y.C. Leung
Department of Mechanical Engineering, The University of Hong Kong, Pokfulam Road, Hong Kong

1. INTRODUCTION

City-scale air pollution is a widely concerned problem because of its adverse impacts on the health of city inhabitants and the associated medical burden on the community. In a city, one of the major sources of air pollutants is vehicular exhaust which emits more than 50% of nitrogen dioxide (NO_2), carbon monoxide (CO) and other organic air pollutants. Vehicular pollutants are mostly emitted on the ground level. It follows the micro-scale wind flow inside the street canyon moving upward to the roof level and eventually being removed to the shear layer. This transport process is complicated by the building configurations and meteorological conditions that has attracted the interests of numerous research studies including field measurements, laboratory experiments and mathematical modeling. More detailed literature reviews are discussed elsewhere (e.g. Vardoulakis et al. 2003; Li et al. 2006).

Cheng et al. (2008) focused on an idealized two-dimensional (2D) street canyon of building-height-to-street wide (aspect) ratio $h/b = 1$ in which they revealed the mechanisms of air (ACH) and pollutant (PCH) exchange rates using steady-state computational fluid dynamics (CFD) solutions under isothermal conditions. In fact, buoyancy, mainly due to the heat dissipation from solar radiation on facades and road surfaces, substantially modifies the structures of wind flow and pollutant transport inside a street canyon (Kim and Baik 1999, 2001; Xie et al. 2006, 2007). In this paper, we are interested in the unsteady-state behaviors, if any, of ventilation and pollutant removal in a street canyon under unstable stratifications. An idealized street canyon of $h/b = 1$ at Reynolds number (Re = $U_0 h/\nu$, where U_0 is the reference wind speed scale and ν the molecular kinematic viscosity) equal to 12,000 serves as a demonstration in this paper to illustrate the unsteady-state nature of ACH and PCH at Richardson number (Ri = $-gh/U_0^2 \times \Delta\Theta/\Theta_0$, where g is the gravitational acceleration, $\Delta\Theta$ the temperature difference and Θ_0 the characteristic temperature scale) equal to -8 and -16.

2. METHODOLOGY

2.1 Mathematical Model

Unlike our previous study (Cheng et al. 2008), the unsteady-state incompressible Reynolds-averaged Navier-Stokes (RANS) equations equipped with the Renormalization Group (RNG) *k-ε* turbulence model (Yakhot et al. 1986) was used. The governing equations consist of the continuity

$$\frac{\partial \overline{u_i}}{\partial x_i} = 0 \tag{1}$$

and the momentum conservation

$$\frac{\partial \overline{u_i}}{\partial t} + \frac{\partial \overline{u_i}\,\overline{u_j}}{\partial x_j} = -\frac{\partial \overline{p}}{\partial x_i} - \frac{\partial \overline{u_i' u_j'}}{\partial x_j} + \delta_{i2}\frac{\overline{\theta} - \Theta_0}{\Theta_0} g \tag{2}$$

Here, t is the time, $\overline{u_i}$ the velocity tensor, x_i the Cartesian coordinate, $\overline{p}$ the kinematic pressure, δ_{ij} the Kronecker delta and $\overline{\theta}$ the air temperature. The tensor $\overline{u_i' u_j'}$ represents the Reynolds stress which is modeled by the eddy-viscosity model

$$\overline{u_i' u_j'} = -\nu_t\left(\frac{\partial \overline{u_i}}{\partial x_j} + \frac{\partial \overline{u_j}}{\partial x_i}\right) - \frac{2}{3}\delta_{ij}k, \tag{3}$$

where ν_t (= $C_\nu k^2/\varepsilon$) is the turbulent kinematic viscosity, C_ν (= 0.0845) the modeling constant, k ($= \overline{u_i' u_i'}/2$) the turbulent kinetic energy (TKE) and ε the TKE dissipation rate. Boussinesq approximation is used in Equation (2) to handle the effects of buoyancy.

Equations (1) and (2) are expressed in tensor notation and the usual summation convention on repeated indices (i, j = 1, 2) applies. A variable with an overline represents the ensemble average while with a prime represents the fluctuating quantity. To account for the thermal effects, the energy conservation

$$\frac{\partial \overline{\theta}}{\partial t} + \frac{\partial \overline{u_i}\,\overline{\theta}}{\partial x_i} = \frac{\partial}{\partial x_i}\left(\kappa_t \frac{\partial \overline{\theta}}{\partial x_i}\right) \tag{4}$$

is considered, where κ_t (= ν_t/Pr_t, where Pr_t = 0.72 is the turbulent Prandtl number) is the turbulent diffusivity of heat. For a passive and inert air pollutant with ensemble averaged concentration $\overline{\phi}$, its transport is represented by the mass conservation

$$\frac{\partial \overline{\phi}}{\partial t} + \frac{\partial \overline{u_i}\,\overline{\phi}}{\partial x_i} = \frac{\partial}{\partial x_i}\left(D_t \frac{\partial \overline{\phi}}{\partial x_i}\right) \tag{5}$$

where D_t (= ν_t/Sc_t, where Sc_t = 0.72 is the turbulent Schmidt number) is the turbulent diffusivity of pollutant.

* *Corresponding author address:* Chun-Ho Liu, Department of Mechanical Engineering, 7/F Haking Wong Building, The University of Hong Kong, Pokfulam Road, Hong Kong; e-mail: liuchunho@graduate.hku.hk

Turbulence of the system is modeled by the RNG k-ε turbulence model which includes the transport of TKE

$$\frac{\partial k}{\partial t}+\frac{\partial \overline{u_i}k}{\partial x_i}=\frac{\partial}{\partial x_i}\left(\alpha_k \nu_t \frac{\partial k}{\partial x_i}\right)+P_k+G_b-\varepsilon \quad (6)$$

and the transport of ε

$$\frac{\partial \varepsilon}{\partial t}+\frac{\partial \overline{u_i}\varepsilon}{\partial x_i}=\frac{\partial}{\partial x_i}\left(\alpha_\varepsilon \nu_t \frac{\partial \varepsilon}{\partial x_i}\right)$$

$$+C_{1\varepsilon}\frac{\varepsilon}{k}\left(P_k+C_{3\varepsilon}G_b\right) \quad . \quad (7)$$

$$-\left[C_{2\varepsilon}+\frac{C_\nu \eta^3\left(1-\eta/\eta_0\right)}{1+\gamma\eta^3}\right]\frac{\varepsilon^2}{k}$$

Here, α_k and α_ε are the inverse effective Prandtl number for k and ε, respectively. In this paper, a flow at high Re is assumed that yields $\alpha_k = \alpha_\varepsilon = 1.393$. The source terms P_k and G_b represent, respectively, the TKE production due to wind shear

$$P_k=\nu_t\left(\frac{\partial \overline{u_i}}{\partial x_j}+\frac{\partial \overline{u_j}}{\partial x_i}\right)\times\frac{\partial \overline{u_i}}{\partial x_j} \quad (8)$$

and buoyancy

$$G_b=-\delta_{i2}\frac{g}{\Theta}\times\frac{\nu_t}{\mathrm{Pr}_t}\times\frac{\partial \overline{\theta}}{\partial x_i} \quad (9)$$

The last term on the right-hand side of Equation (7) is

$$\eta=\frac{k}{\varepsilon}\sqrt{\left(\frac{\partial \overline{u_i}}{\partial x_j}+\frac{\partial \overline{u_j}}{\partial x_i}\right)\frac{\partial \overline{u_i}}{\partial x_j}} \; . \quad (10)$$

The modeling constants for the RNG ***k-ε*** turbulence model are $\eta_0 = 4.38$, $\gamma = 0.012$, $C_{1\varepsilon} = 1.42$, $C_{2\varepsilon} = 1.68$ and $C_{3\varepsilon}$ = $\tanh|w/v|$, where w is the vertical and v the horizontal velocity components.

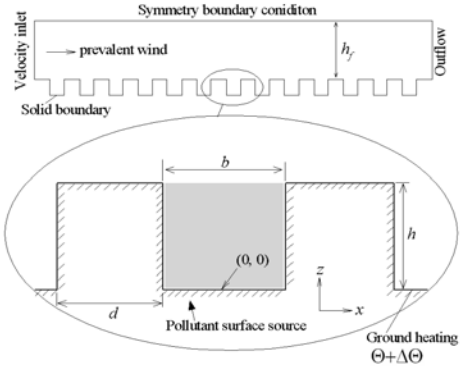

Figure 1. Computational domain and boundary conditions for the combined wind-buoyancy driven wind flow and pollutant transport in street canyons. The shaded region is the volume Ω of center street canyon.

2.2 Computational Domain & Boundary Conditions

The 2D computational domain consists of 13 identical street canyons of $h/b = 1$ regularly placed under the shear layer (Figure 1). Only the wind flow and pollutant transport in the center street canyon is examined while the rest of the street canyons are used to facilitate fully developed turbulence in the core of the computational domain (Meroney et al. 1996).

At the top of the shear layer, $h_f = 3h$ measuring from the roof of the street canopy, is prescribed as symmetry boundary at constant temperature Θ. The prevalent wind in the shear layer is driven by an inflow boundary at the upstream inlet and an outflow boundary at the downstream outflow. The inflow (vertical) wind profile is

$$U(z)=\mathrm{U}_0\left(\frac{z}{h_f+h}\right)^\alpha \; , \quad (11)$$

also known as the power law, where α (= 0.28) is the wind profile exponent and z the ground-normal distance. To account for the effects of (unstable) stratification, all the streets are heated at a uniform temperature (Θ+ΔΘ) to activate unstable stratifications. In addition, a linear (decreasing) temperature profile

$$\Theta(z)=\Theta+\Delta\Theta\left(1-\frac{z}{h}\right) \quad (12)$$

is prescribed at all the building facades. No-slip boundaries are used on all the solid boundaries (roofs, facades and streets). A uniform area pollutant source with constant pollutant concentration C_0 is placed on the ground surface of the center street canyon.

The wind flow is characterized by the dimensionless parameters Prandtl number (Pr), Re and Ri. In this paper, Pr and Re are kept constant at 0.72 and 12,000, respectively, that are high enough for flow independent from molecular viscosity (Pavageau and Schatzmann 1999). Whilst, Ri measures the relative driving forces of wind and buoyancy to the flow that is controlled by adjusting g. The aspect ratio of the street canyon is kept constant at $h/b = 1$.

Over 2 million triangular elements were used to discretize the 2D computational domain. Given h^2 the cross-sectional area of the street canyon of $h/b = 1$, the minimum and maximum sizes of the element are approximately $10^{-7}h^2$ and $10^{-3}h^2$, respectively. The 3rd-order-accurate monotone upstream-centered scheme for conservation law (MUSCL) was used in the spatial domain while the implicit 1st-order-accurate PISO scheme was used in the temporal domain.

3. FORMULATIONS OF ACH & PCH

Cheng et al. (2008) developed the mathematical formulations of ACH and PCH based on the eddy-viscosity and -diffusivity models for a systematic comparison of ventilation and air quality in street canyons. This section summarizes those formulations.

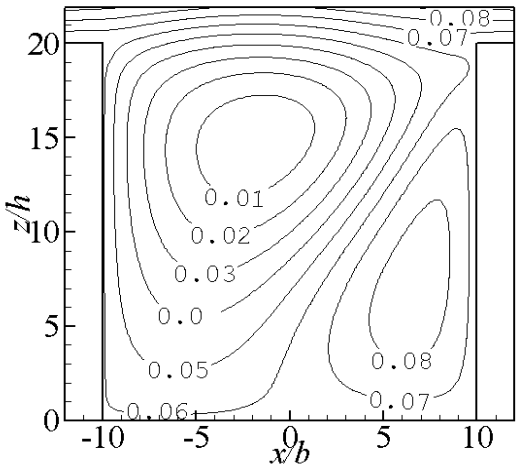

Figure 2. Streamlines of the street canyon at Ri = -8.

3.1 Air Exchange Rate (ACH)

ACH represents the rate of air removal from a street canyon through the roof level. It is defined as

$$\mathrm{ACH} = \frac{1}{\lambda}\int_0^{\lambda}\int_{\Gamma_{\mathrm{roof}}} w_+ \, dxdt \,. \tag{13}$$

Here, w is the vertical velocity component, Γ_{roof} the roof area of the street canyon and λ the sampling time. The subscript + signifies that only the upward wind flow $w > 0$ is taken into account. The ACH in Equation (13) can be further partitioned into its mean ($\overline{\mathrm{ACH}}$) and turbulence (ACH') components in the form

$$\mathrm{ACH} = \overline{\mathrm{ACH}} + \mathrm{ACH}'. \tag{14}$$

$\overline{\mathrm{ACH}}$ can be calculated by the mean flow

$$\overline{\mathrm{ACH}} = \int_{\Gamma_{\mathrm{roof}}} \overline{w}_+ \, dx \tag{15}$$

while ACH' can be calculated by assuming isotropic turbulence and using the eddy-viscosity model

$$\begin{aligned}\mathrm{ACH}' &= \int_{\Gamma_{\mathrm{roof}}} \frac{1}{2}\sqrt{\overline{w'w'}}\, dx \\ &= \int_{\Gamma_{\mathrm{roof}}} \sqrt{\frac{k}{6} - \frac{1}{2}\nu_t \frac{\partial \overline{w}}{\partial z}}\, dx\end{aligned} \,. \tag{16}$$

3.2 Pollutant Exchange Rate (PCH)

PCH, which represents the rate of pollutant removal from a street canyon through the roof level, can be defined in a manner similar to ACH

$$\mathrm{PCH} = \frac{1}{\lambda}\int_0^{\lambda}\int_{\Gamma_{\mathrm{roof}}} wc \, dxdt \tag{17}$$

where wc is the vertical pollutant flux normal to the roof of street canyon. Analogously, PCH can be divided into its mean ($\overline{\mathrm{PCH}}$) and turbulent (PCH') components

$$\mathrm{PCH} = \overline{\mathrm{PCH}} + \mathrm{PCH}'. \tag{18}$$

$\overline{\mathrm{PCH}}$ is calculated by the mean vertical pollutant flux

$$\overline{\mathrm{PCH}} = \int_{\Gamma_{\mathrm{roof}}} \overline{wc}\, dx \tag{19}$$

while PCH' is calculated by the eddy-diffusivity model

$$\mathrm{PCH}' = \int_{\Gamma_{\mathrm{roof}}} \overline{w'c'}\, dx = -\int_{\Gamma_{\mathrm{roof}}} D_t \frac{\partial \overline{c}}{\partial z}\, dx \,. \tag{20}$$

4. RESULTS & DISCUSSIONS

In this section, we report the CFD results for the ventilation and pollutant removal for the street canyon of $h/b = 1$ at Re = 12,000. In particular, the periodic behaviors at Ri = -8 and -16 are contrasted.

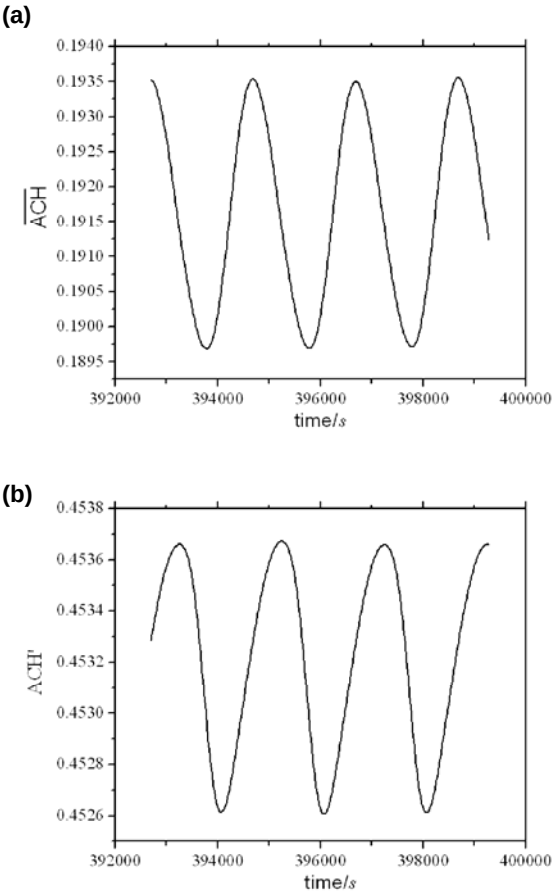

Figure 3. Time traces of (a) $\overline{\mathrm{ACH}}$ and (b) ACH' at Ri = -8.

4.1 Ri = -8

Figure 2 shows the snapshot of streamlines inside the street canyon at Ri = -8 (slightly unstable). For prevalent wind flows from the left-hand side to the right-hand side, a large clockwise-rotating primary recirculation together with another small counter-clockwise-rotating secondary recirculation are formed, respectively, at the center core and the ground-level windward corner of the street canyon. Moreover, buoyancy promotes both the mean and fluctuating winds inside the street canyons. Not shown in this paper are the streamlines under isothermal conditions in which the primary recirculation centered in the street canyon dominates the flow.

In this paper, one of the major findings of the ventilation and pollutant transport inside a street canyon under unstable stratifications is the perturbed wind flow. At sufficiently high Ri (= -8 as determined in this study), the wind flow is no longer steady-state, Instead, the ventilation exhibits periodic ACH in which the period is about λ = 2,200 sec. We decompose the time trace of ACH into the mean ($\overline{\mathrm{ACH}}$; Figure 3a) and turbulent (ACH'; Figure 3b) components. Both ACHs are positive so that no large-scale fresh air entry is calculated by the CFD. ACH' (= 0.4531) is larger than $\overline{\mathrm{ACH}}$ (= 0.1915) by more than 2 times that is in line with our previous finding under isothermal conditions. The amplitude of the periodic $\overline{\mathrm{ACH}}$ (= 4.0×10^{-3}) is larger than that of the periodic ACH' (= 1.1×10^{-3}) by almost three times. This finding signifies the predominant contribution of buoyancy to the mean flow. It is also worth mentioning that a time lag (about 200 sec) is observed in-between the peaks of $\overline{\mathrm{ACH}}$ and ACH'.

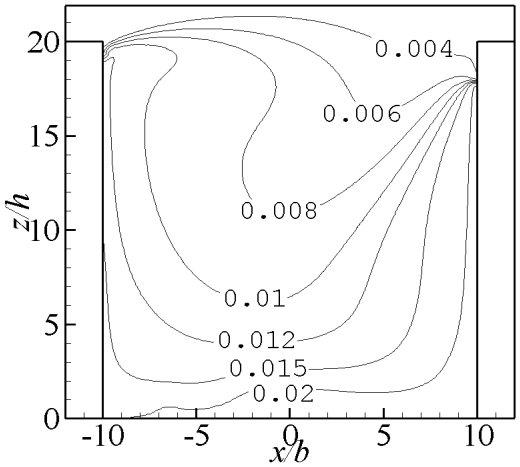

Figure 4. Pollutant distribution at Ri = -8.

Figure 4 depicts the snapshot of the spatial contours of pollutant concentration inside the street canyon at Ri = -8. Because of the uniform ground-level area pollutant source, the pollutant is distributed quite evenly in the near-ground region. Higher pollutant concentrations are observed on both the leeward and windward facades that are caused by the characteristic recirculating wind. Because of the clockwise-rotating primary recirculation, the pollutant is carried toward the leeward facades once emitted from the source. Next, it travels upward along the leeward facade to the roof level resulting in the (slightly) elevated pollutant concentration near the roof-level leeward corner. The aged air and pollutant are then removed from the street canyon to the shear layer (mainly on the leeward side). Simultaneously, the fresh air from the shear layer enters the street canyon that leads to a lower pollutant concentration on the windward side of the street canyon.

Indeed, the pollutant concentration inside the counter-clockwise-rotating secondary recirculation is higher (comparable to that on the ground-level) due to its isolated nature (from the prevalent wind in the shear layer) and the weaker turbulent transport in-between the recirculations. The pollutant thus accumulates on the windward façade leading to prolonged retention time.

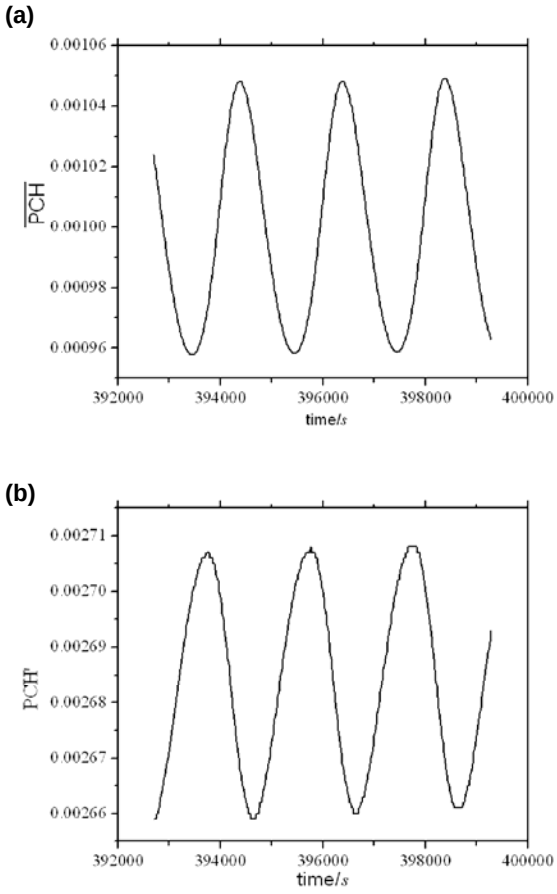

Figure 5. Time traces of (a) $\overline{\mathrm{PCH}}$ and (b) PCH' at Ri = -8.

Because the wind is the carrier of the pollutant, the pollutant transport and removal are unsteady-state in nature. $\overline{PCH}$ and PCH' are calculated by Equations (19) and (20), respectively, at Ri = -8. Figure 5 shows the time traces of the PCHs. Similar to the ventilation at the same Ri, the pollutant removal attributed to the mean component ($\overline{PCH} = 0.001$; Figure 5a) is much smaller (> 2 times) than that of the turbulent component ($PCH' = 0.002685$; Figure 5b). On the contrary, the magnitude of the periodic $\overline{PCH}$ (= 9×10^{-5}) is larger than its PCH' (= 4.5×10^{-5}) counterpart by two folds.

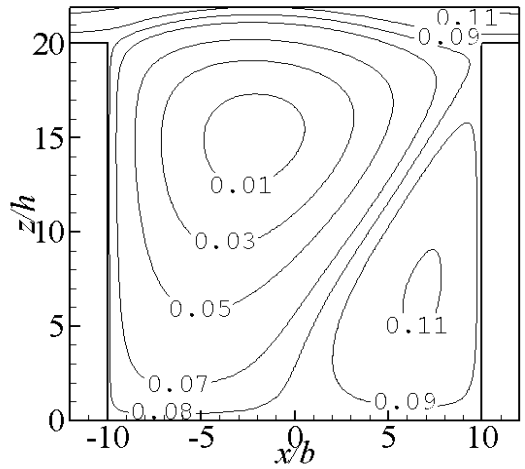

Figure 6. Streamlines of the street canyon at Ri = -16.

4.2 Ri = -16

Next, we double the Ri to -16 for mildly unstable stratifications. Heating up the street canyon to Ri = -16 makes the stratification more unstable. Figure 6 depicts the streamlines inside the street canyon at Ri = -16. Similar to its Ri = -8 counterpart, two counter-rotating recirculations are developed. The primary one leans slightly to the leeward side connecting to the prevalent wind in the shear layer. The secondary recirculation is an isolated one resided at the ground-level windward corner. As expected, buoyancy promotes both the mean and fluctuating winds in the street canyon which can be reflected from the larger streamfunction (and gradient).

The time traces of ACHs at Ri = -16 also exhibit periodic behaviors whose period is about λ = 1,800 sec (Figure 7). Buoyancy not only activates the periodic ventilation but decreasing Ri (increasing $\Delta\Theta$) also shortens the period of oscillation. $\overline{ACH}$ has not well developed yet but the average value is about 0.3093 (Figure 7a). Whereas, the turbulent component ACH' has developed almost fully in which the mean value is about 0.672 (Figure 7b). The amplitudes of periodic $\overline{ACH}$ and ACH' are, respectively, 5.0×10^{-5} and 3.5×10^{-5}. Hence, buoyancy has predominant effect on mean wind.

Figure 8 shows the spatial distribution of pollutant inside the street canyon at Ri = -16. It is similar to that at Ri = -8 because of the similar recirculating structures. Owing to the larger values of ACH and PCH at Ri = -16, the roof-level pollutant concentration is slightly lower. It is thus suggested that buoyancy favors ventilation and pollutant removal.

Periodic behaviors are also observed in the PCHs of street canyon at Ri = -16 (Figure 9). $\overline{PCH}$ (=1.88×10^{-3}) lags slightly behinds PCH' (= 2.18×10^{-3}). Similar to other ACHs and PCHs reported previously, the amplitude of periodic $\overline{PCH}$ (= 4.5×10^{-5}) is larger than that of PCH' (= 2×10^{-5}) by more than two times that again suggests the predominant contribution of buoyancy to the mean flow.

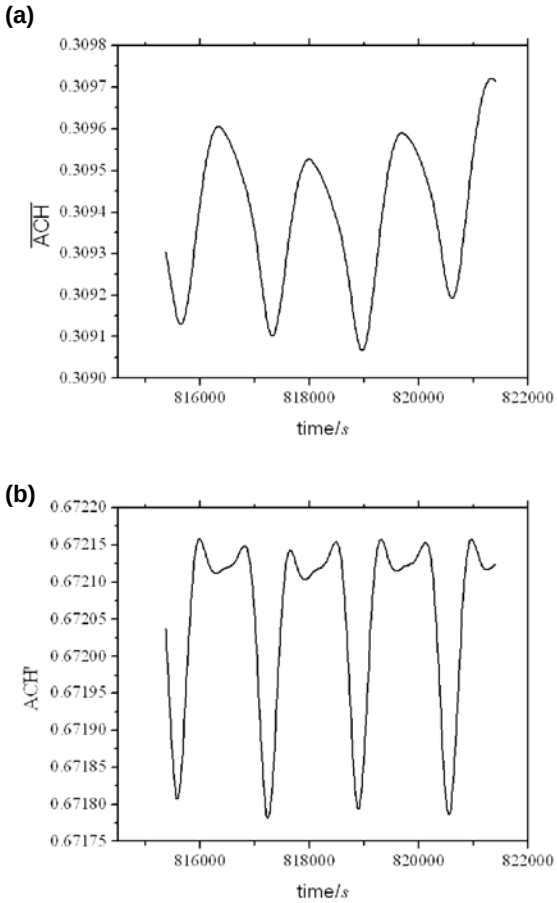

Figure 7. Time traces of (a) $\overline{ACH}$ and (b) ACH' at Ri = -16.

5. CONCLUSIONS

The mechanisms of ventilation and pollutant removal for 2D street canyons of $h/b = 1$ under unstable stratification (Ri = -8 and -16) with all the building roofs, facades and streets being heating up were studied using the RNG k-ε turbulence model. In particular, we focused on the periodic behaviors of ventilation and pollutant removal induced by buoyancy. CFD results shows that two counter-rotating recirculations are developed inside the street canyon. Buoyancy favors ventilation and so does pollutant removal at large. However, the isolated nature of the secondary recirculation leads to an locally elevated pollutant concentration on the windward façade. Buoyancy promotes the unsteady-state ACHs and PCHs as well in which the amplitudes of the periodic ACHs and PCHs are found to increase with increasing Ri.

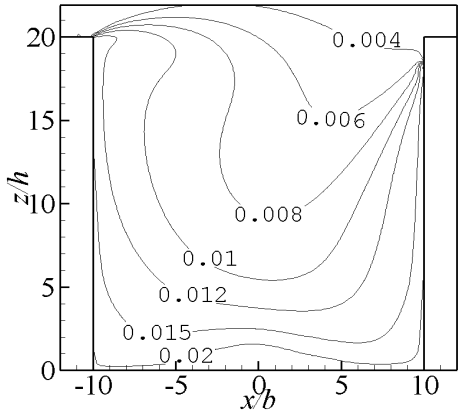

Figure 8. Pollutant distribution at Ri = -16.

6. REFERENCES

Cheng, W.C., Liu, C.-H. and Leung, D.Y.C., 2008: Computational formulation for the evaluation of street canyon ventilation and pollutant removal performance. *Atmo. Environ.*, 42, 9041-9051.

Kim, J.-J. and Baik, J.-J., 1999: A numerical study of thermal effects on flow and pollutant dispersion in urban street canyon. *J. Appl. Meteorol.*, 38, 1249-1261.

Kim, J.-J. and Baik, J.-J., 2001: Urban street-canyon flows with bottom heating. *Atmo Environ.*, 35, 3395-3404.

Li, X.-X., Liu, C.-H., Leung, D.Y.C. and Lam, K.M., 2006: Recent progress in CFD modelling of wind field and pollutant transport in street canyons. *Atmo. Environ.*, 40, 5640-5658.

Meroney, R.N., Pavageau, M., Rafailidis, S. and Schatzmann, M., 1996: Study of line source characteristics for 2-D physical modeling of pollutant dispersion in street canyons. *J. Wind Eng. Ind. Aerodyn.*, 62, 37-56.

Pavageau, M. and Schatzmann, M., 1999: Wind tunnel measurements of concentration fluctuations in an urban street canyon. *Atmo. Environ.*, 33, 3961-3971.

Vardoulakis, S., Fisher, B.E.A., Pericleous, K. and Gonzalez-Flesca, N., 2003: Modelling air quality in street canyons: a review, *Atmo. Environ.*, 37, 155-182.

Xie, X., Liu, C.-H., Leung, D.Y.C. and Leung, M.K.H., 2006: Characteristics of air exchange in a street canyon with ground heating. *Atmo. Environ.*, 40, 6396-6409.

Xie, X., Liu, C.-H. and Leung, D.Y.C., 2007: Impact of building facades and ground heating on wind flow and pollutant transport in street canyons. *Atmo. Environ.*, 41, 9030-9049.

Yakhot, V., Orszag, S.A., Thangam, S., Gatski, T.B. and Speziale, C.G., 1986: Renormalization group analysis of turbulence. *J. Sci. Comput.*, 1, 3-51.

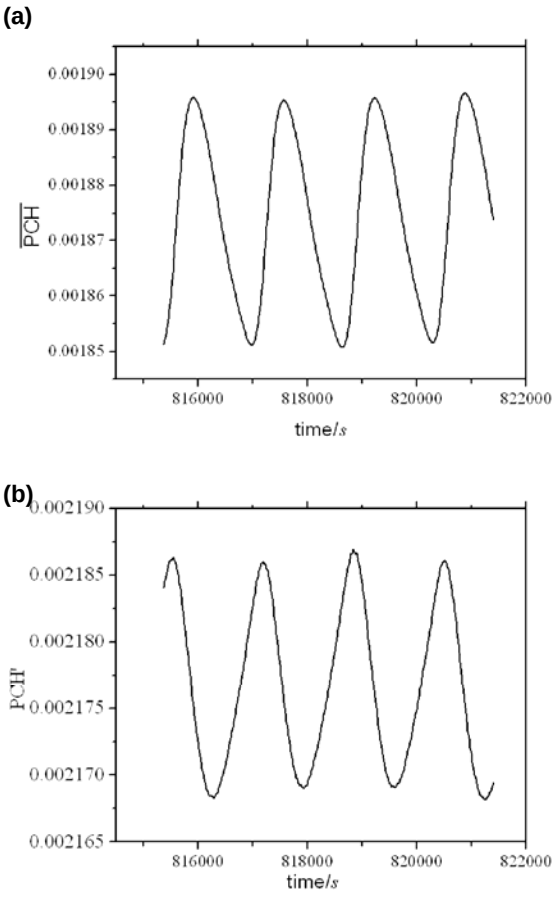

Figure 9. Time traces of (a) $\overline{\mathrm{PCH}}$ and (b) PCH' at Ri = -16.